

Ab-initio theory of CPP transport

P. Weinberger

Center for Computational Materials Science
TU Wien, Getreidemarkt 6/134, A1060 Vienna, Austria

Abstract

The phenomenon of electric transport perpendicular to the planes of atoms is discussed in terms of an ab-initio approach based on the Kubo-Greenwood equation. Since level of description is fully relativistic “artifacts” due to spin resolution are avoided. Besides a formal discussion of the applied methods and an illustration of the numerical procedures, in particular the dependence of the magnetoresistance on the quality of interfaces, and issues concerning “tunneling” in metal/non-metal heterojunctions are discussed.

1 Introduction

Although current perpendicular to the planes of atoms (CPP) experiments seem to be easy to visualize in terms of a Landauer-type view of electric transport, its theoretical description poses quite a few questions. Is it sufficient to consider transmission and reflection matrices placed only at planes well-situated within the leads? What is the relationship between conductivity and resistivity? Which part of a heterojunction, spacer or interfaces actually causes a sufficiently large magnetoresistance ratio? If it is the spacer, how much matters its actual structure? If the magnetoresistance is mainly due to the interfaces, how about experimentally unavoidable interdiffusion? Are there any criteria in terms of the resistivity or resistance other than rules of thumb that would distinguish between “tunneling” and “weak” metallic conductance? Clearly enough on top of all these questions nags the doubt whether or not it is justified to consider “spin” as an observable, i.e., whether or not the concept of “spin currents” (spin-resolved currents) makes any sense.

In this contribution exclusively the Kubo-Greenwood equation [1, 2, 3, 4] is applied to CPP. Furthermore, in all applications and illustration shown a fully relativistic realization of this equation is used implying that right from the beginning “spin” will not be considered as an independent (“observable”) quantity. As recently two review articles appeared [5, 6] discussing various aspects of the “giant magnetoresistance” (GMR), including also CPP concepts, no attempt is made to present in here also other ab-initio type approaches. For a very detailed discussion of all theoretical implications of the present approach such

as collinearity and non-collinearity, magnetic configurations, inhomogeneous alloying, etc., the reader is referred to a forthcoming review article [11].

2 The relativistic Kubo-Greenwood equation for systems with two-dimensional translational symmetry

Within the (non-relativistic) Density Functional Theory (DFT) the Kohn-Sham-Dirac Hamiltonian is given by

$$\mathcal{H} = \boldsymbol{\alpha} \cdot \mathbf{p} + \beta mc^2 + V^{eff} [n, \mathbf{m}] + \beta \boldsymbol{\Sigma} \cdot \mathbf{B}^{eff} [n, \mathbf{m}] \quad , \quad (1)$$

$$\begin{aligned} \alpha_i &= \begin{pmatrix} 0 & \sigma_i \\ \sigma_i & 0 \end{pmatrix} \quad , \quad \beta = \begin{pmatrix} I_2 & 0 \\ 0 & -I_2 \end{pmatrix} \quad , \\ \Sigma_i &= \begin{pmatrix} \sigma_i & 0 \\ 0 & \sigma_i \end{pmatrix} \quad , \quad I_2 = \begin{pmatrix} 1 & 0 \\ 0 & 1 \end{pmatrix} \quad , \end{aligned} \quad (2)$$

$$V(\mathbf{r}) \equiv V^{eff} [n, \mathbf{m}] = V^{ext} + V^{Hartree} + \frac{\delta E_{xc}[n, \mathbf{m}]}{\delta n} \quad , \quad (3)$$

$$\mathbf{B}(\mathbf{r}) \equiv \mathbf{B}^{eff} [n, \mathbf{m}] = \mathbf{B}^{ext} + \frac{e\hbar}{2mc} \frac{\delta E_{xc}[n, \mathbf{m}]}{\delta \mathbf{m}} \quad , \quad (4)$$

where n is the particle density, \mathbf{m} the magnetization density, $V^{eff} [n, \mathbf{m}]$ the effective potential, $\mathbf{B}^{eff} [n, \mathbf{m}]$ the effective (exchange) magnetic field, V^{ext} and \mathbf{B}^{ext} the corresponding external fields, and the α_i are Dirac- and the σ_i Pauli (spin) matrices, see also refs. [7, 8].

If $G(z)$ denotes the resolvent of this Hamiltonian,

$$G(z) = (z - \mathcal{H})^{-1} \quad , \quad z = \epsilon + i\delta \quad , \quad (5)$$

then within the Kubo-Greenwood equation [1, 2, 3, 4] the diagonal elements of the conductivity tensor are defined as

$$\sigma_{\mu\mu} = \frac{\hbar}{\pi N_0} \text{tr}_{at} \left\langle J_\mu \text{Im} G^+(\epsilon_F) J_\mu \text{Im} G^+(\epsilon_F) \right\rangle \quad , \quad (6)$$

where $\text{Im} G^+(\epsilon)$,

$$\text{Im} G^+(\epsilon) = \frac{1}{2i} (G^+(\epsilon) - G^-(\epsilon)) \quad , \quad (7)$$

can be formulated in terms of the so-called side-limits of $G(z)$,

$$\lim_{|\delta| \rightarrow 0} G(z) = \begin{cases} G^+(\epsilon) & ; \delta > 0 \\ G^-(\epsilon) & ; \delta < 0 \end{cases} \quad . \quad (8)$$

Usually multiple scattering theory [8, 9] is applied in order to evaluate $G(z)$ in the configuration space representation (Green's function) and to perform the trace in eqn. (6). If the system under consideration can be characterized by two-dimensional translational symmetry (layered system; one and the same translational invariance has to apply in all atomic layers) then for a particular magnetic configuration \mathcal{C} the diagonal elements of the conductivity tensor can be written [10, 11] as a double sum over atomic layers,

$$\sigma_{\mu\mu}(\mathcal{C}; n) = \frac{1}{n} \sum_{p,q=1}^n \sigma_{\mu\mu}^{pq}(\mathcal{C}; n) \quad , \quad (9)$$

where

$$\sigma_{\mu\mu}^{pq}(\mathcal{C}; n) = \lim_{\delta \rightarrow 0} \sigma_{\mu\mu}^{pq}(\mathcal{C}; n; \delta) \quad , \quad (10)$$

$$\sigma_{\mu\mu}^{pq}(\mathcal{C}; n; \delta) = \frac{1}{4} \sum_{i,j=1}^2 (-1)^{i+j} \sigma_{\mu\mu}^{pq}(\mathcal{C}; \epsilon_i, \epsilon_j; n) \quad , \quad (11)$$

and n denotes the total number of atomic layers taken into account.

3 Current-perpendicular to the planes of atoms (CPP)

Let z and z' denote continuous coordinate variables perpendicular to the planes of atoms in a two-dimensional translationally invariant system. In the steady state one can write the resistivity in the current-perpendicular to the planes of atoms geometry (CPP) as [12, 13]

$$\rho_{CPP} = \frac{1}{L} \int \rho(z, z') dz dz' \quad , \quad (12)$$

where $\rho(z, z')$ is the inverse of $\sigma(z, z')$ as defined by

$$\int \sigma(z, z'') \rho(z'', z') dz'' = \delta(z - z') \quad , \quad (13)$$

and L is the overall length of the structure for which the conductivity is calculated, see also ref. [14]. The sheet resistance r and resistance R are then defined by the following relations

$$r = AR = L\rho_{CPP} = \int \rho(z, z') dz dz' \quad , \quad (14)$$

where A is the unit area.

The conductivity tensor $\sigma(z, z')$ can now be mapped [15] (f :) onto the zz -components of the conductivity tensor for a layered system introduced earlier, $\sigma_{zz}^{ij}(n) \equiv \sigma_{ij}(n)$, $i, j = 1, n$, with i and j denoting planes of atoms,

$$f : \sigma(z, z') \rightarrow \sigma_{ij}(n) \quad , \quad (15)$$

such that the algebraic structure established by eqn. (13) is conserved,

$$\sum_{k=1}^n \rho_{ik}(n) \sigma_{kj}(n) = \delta_{ij} \quad . \quad (16)$$

Clearly enough the sheet resistance r in eqn. (14) then serves as measure (g :) for the mapping f ,

$$g : r \rightarrow r(n) \quad , \quad r(n) = \sum_{i,j=1}^n \rho_{ij}(n) \quad , \quad (17)$$

since according to the Cauchy convergence criterion the integral in eqn. (14) can be mapped onto a sum, i.e., onto $r(n)$, if and only if,

$$\left| r - \lim_{n \rightarrow \infty} r(n) \right| < \Delta \quad , \quad n \in \mathbb{N}^+ \quad , \quad (18)$$

or,

$$|r(n+m) - r(n)| < \Delta; \quad n, m \in \mathbb{N}^+ \quad , \quad (19)$$

where Δ is an infinitesimal small number.

Making use of complex Fermi energies, $\mathcal{E}_F = \epsilon_F \pm i\delta$, according to eqn. (8) the sheet resistance for a given magnetic configuration \mathcal{C} is defined by

$$r(\mathcal{C}; n) = \lim_{\delta \rightarrow 0} r(\mathcal{C}; n; \delta) \quad , \quad (20)$$

where

$$r(\mathcal{C}; n; \delta) = \sum_{i,j=1}^n \rho_{ij}(\mathcal{C}; n; \delta) \quad , \quad (21)$$

and

$$\sum_{k=1}^n \rho_{ik}(\mathcal{C}; n; \delta) \sigma_{kj}(\mathcal{C}; n; \delta) = \delta_{ij} \quad . \quad (22)$$

It should be noted that eqn. (20) simply refers to the side limiting procedure in eqn. (8).

4 CPP transport in heterojunctions

Suppose now for matters of simplicity that a typical heterojunction consists of n atomic layers of magnetic leads (L) and s atomic layers of a spacer X, i.e., suppose that a heterojunction is of the type $L_n X_s L_n$. The total number of atomic layers t amounts therefore to $t = 2n + s$ which in turn implies for a given number of spacer layers that the convergence criterion in eqn. (19) reads as follows

$$|r(\mathcal{C}; 2(n+m) + s) - r(\mathcal{C}; 2n + s)| < \Delta \quad , \quad m, n \in \mathbb{N}^+ \quad . \quad (23)$$

For each given spacer thickness s , the sheet resistance corresponding to a particular magnetic configuration \mathcal{C} is therefore given by

$$r(\mathcal{C}; s) = \lim_{m \rightarrow M} \lim_{\delta \rightarrow 0} r(\mathcal{C}; 2(n + m) + s; \delta) \quad . \quad (24)$$

where M is a sufficiently large integer number. In practical terms eqn. (24) can be split up into two independent limiting procedures,

$$r(\mathcal{C}; s; \delta) = \lim_{m \rightarrow M} r(\mathcal{C}; 2(n + m) + s; \delta) \quad , \quad (25)$$

$$r(\mathcal{C}; s) = \lim_{\delta \rightarrow 0} r(\mathcal{C}; s; \delta) \quad . \quad (26)$$

4.1 Magnetoresistance ratio

The magnetoresistance ratio MR (GMR , “giant magnetoresistance”) corresponds in the so-called “pessimistic view” to

$$MR = \frac{r(\mathcal{C}'; s) - r(\mathcal{C}; s)}{r(\mathcal{C}'; s)} \quad , \quad (27)$$

and in the “optimistic view” to

$$MR = \frac{r(\mathcal{C}'; s) - r(\mathcal{C}; s)}{r(\mathcal{C}; s)} \quad , \quad (28)$$

where in the case of collinear magnetic configurations \mathcal{C} and \mathcal{C}' usually are termed “parallel” and “antiparallel” configuration. The advantage of the definition in eqn. (27) is simply that thus the magnetoresistance ratio is bound by one. Unfortunately experimental data very often refer rather to the second kind of definition (because the value of the giant magnetoresistance ratio is larger?). It should be noted in this context, however, that eqn. (27) corresponds to the only useful definition of the angular dependence of the anisotropic magnetoresistance. In here exclusively the “pessimistic view” is used.

4.2 Physical significance of the imaginary part of the Fermi energy

Suppose that in the Kubo-Greenwood equation, see (6), the current operator can be approximated by a constant,

$$\bar{\sigma} \sim tr \quad \text{Im} G^+(\epsilon_F) \text{Im} G^+(\epsilon_F) \rangle \sim n^2(\epsilon_F) \quad , \quad (29)$$

which in turn implies that the sheet resistance can approximately be written as

$$\bar{r} = L\bar{\sigma}^{-1} = Ln^{-2}(\epsilon_F) \quad . \quad (30)$$

Furthermore, suppose the density of states is calculated for complex Fermi energies, $\mathcal{E}_F = \epsilon_F + i\delta$,

$$\bar{r}(\delta) = L\bar{\sigma}^{-1} = Ln^{-2}(\epsilon_F + i\delta) \quad , \quad (31)$$

then from the properties of the density of states,

$$\frac{d[n(\epsilon_F + i\delta)]}{d\delta} = \begin{cases} > 0; & \text{“non-metallic”} \\ < 0; & \text{“metallic”} \end{cases} \quad , \quad (32)$$

follows immediately

$$\frac{d[\bar{r}(\delta)]}{d\delta} = \begin{cases} > 0; & \text{“metallic”} \\ < 0; & \text{“non-metallic”} \end{cases} \quad . \quad (33)$$

The functional form of the actually calculated sheet resistance with respect to the imaginary part of the Fermi energy, see eqns. (25) and (26), can therefore be used to qualitatively interpret the underlying type of conduction

$$\frac{d[r(\mathcal{C}; s; \delta)]}{d\delta} = \begin{cases} > 0; & \text{“metallic”} \\ < 0; & \text{“non-metallic”} \end{cases} \quad . \quad (34)$$

The last equation means *inter alia* that in the case of a negative slope of the sheet resistance with respect to δ “tunneling” might occur. The parameter δ obviously acts like a (small) constant selfenergy: in the regime of metallic conduction an increase of the selfenergy implies an increased resistivity (sheet resistance); in the non-metallic regime an increase of δ reduces the resistance, the system becomes more metallic.

Since very often the actual composition of a heterostructure is not known, i.e., no information about interdiffusion at the interfaces, macroscopic roughness, etc., are not available, in such a case it seems sufficient to consider the following magnetoresistance ratio,

$$MR(\delta) = \frac{r(\mathcal{C}'; s; \delta) - r(\mathcal{C}; s; \delta)}{r(\mathcal{C}'; s; \delta)} \quad , \quad (35)$$

where δ is sufficiently small, for a semi-quantitative characterization.

5 CPP transport & IEC

Certain aspects of current-in-plane (CIP) and CPP electric transport have to be correlated with the so-called interlayer exchange coupling energy (IEC). The IEC classifies the type of coupling between the magnetic parts of a heterojunction, i.e., determines regimes of parallel and antiparallel coupling, or, can serve as (continuous) energy variable in an ab-initio description of the exchange bias in spin valve systems [16].

Up to now in most evaluations of the IEC the magnetic force theorem [17] was applied by considering the grand-potentials of the two magnetic configurations under investigation

$$\Delta E_b = E_b(\mathcal{C}) - E_b(\mathcal{C}_0) \quad , \quad (36)$$

evaluating, however, only one magnetic configuration (\mathcal{C}_0 , one of them) selfconsistently. If c_α^p denotes the respective concentrations of the constituents A and B in layer p then in terms of the (inhomogeneous) CPA for layered systems [10], ΔE_b is given by

$$\Delta E_b = \sum_{p=1}^N \sum_{\alpha=A,B} c_\alpha^p \Delta E_\alpha^p \quad , \quad \sum_{\alpha=A,B} c_\alpha^p = 1 \quad , \quad (37)$$

where the

$$\Delta E_\alpha^p = \int_{\epsilon_b}^{\epsilon_F} (n_\alpha^p(\mathcal{C}, \epsilon) - n_\alpha^p(\mathcal{C}_0, \epsilon)) (\epsilon - \epsilon_F) d\epsilon \quad , \quad (38)$$

refer to component- and layer-resolved contributions to the grand-potential at $T=0$. In eqn. (38) the $n_\alpha^p(\mathcal{C}, \epsilon)$ are component and layer projected DOS's corresponding to magnetic configuration \mathcal{C} , ϵ_b denotes the bottom of the valence band and ϵ_F is the Fermi energy of the (nonmagnetic) substrate, see also ref. [8]. The energy integral in eqn. (38) is usually performed in the upper half of the complex plane using a contour starting at ϵ_b and ending at ϵ_F .

Note that because of the definition given in eqn. (36) this implies the following energetic order of magnetic configurations

$$\Delta E_b = \begin{cases} > 0; & \rightarrow \mathcal{C}; \text{ preferred configuration} \\ < 0; & \rightarrow \mathcal{C}_0; \text{ preferred configuration} \end{cases} \quad . \quad (39)$$

6 Numerical implementation

All examples and illustrations shown in here are based on applications of the fully relativistic versions of the Screened Korringa-Kohn-Rostoker (SKKR) method [8] and the Kubo-Greenwood equation [11]. Disorder such as interdiffusion at interfaces or alloying in the spacer part is described in terms of the (inhomogeneous) Coherent Potential Approximation (CPA) for layered systems [10].

7 Illustrations of the numerical procedures

In Fig. 1 the variation of the parallel (\mathcal{P}) and antiparallel (\mathcal{AP}) sheet resistance in bcc-Fe(100)/Fe $_n$ Ge $_s$ Fe $_n$ /Fe(100) is shown for a particular value of δ and s versus the number of Fe lead layers. As can be seen for $n > 8$ the sheet resistances start to grow linearly with n . For $\delta \rightarrow 0$ the slope in this linear regime tends to zero [15], i.e., for a sufficient number of lead layers the sheet resistances become constant: the requirements in eqns. (25) and (26). The physical reason for the convergence properties with respect to the number of lead layers has to be correlated [15] with the oscillations of the (layer-resolved) Madelung potentials, which starting at the interface only slowly approach the Madelung potential in pure bcc-Fe(100).

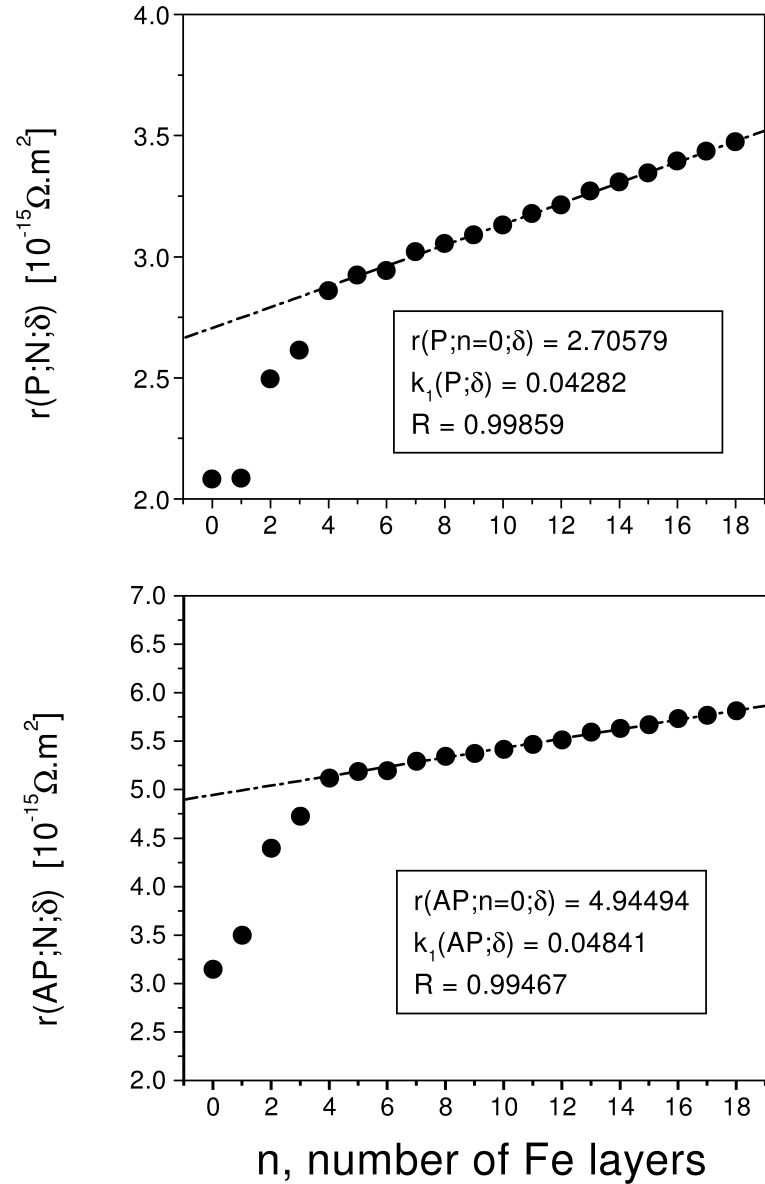


Figure 1: Variation of the sheet resistance $r(\mathcal{C}; n; \delta)$ for bcc Fe(100)/Fe_nGe_sFe_n/Fe, $\delta = 2$ mry, $s = 9$, with respect to n . The upper panel refers to the parallel configuration, the lower to the antiferromagnetic configuration. Dashed lines indicate the extrapolation of the linear regime to $n = 0$. From ref. [15].

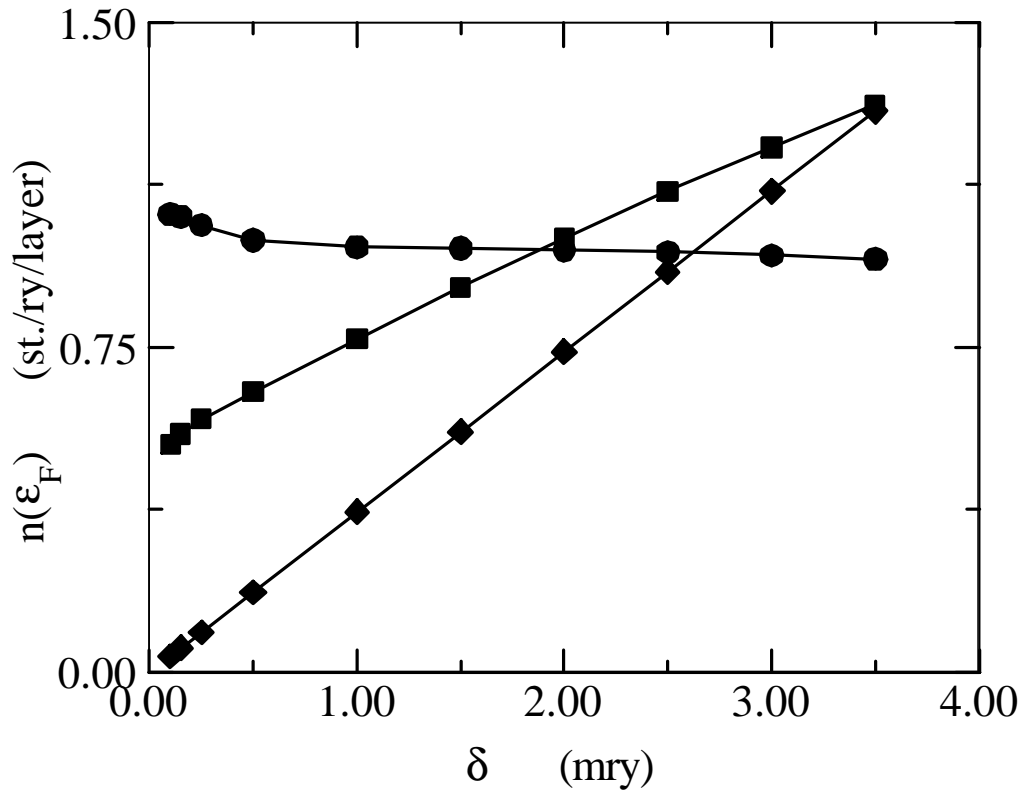


Figure 2: Density of states of the center vacuum layer at the complex Fermi energy $\epsilon_F + i\delta$ as a function of δ in bcc-Fe(100)/Fe₁₂Vac_sFe₁₂/Fe(100) for $s = 3$ (circles), $s = 6$ (squares; multiplied by 100), and $s = 9$ (diamonds; multiplied by 250). From ref. [18].

In Fig. 2 the density of states of bcc-Fe/Fe_nVac_sFe_n/Fe(100) at the Fermi level is displayed with respect to δ for 3, 6 and 9 layers of vacuum separating bcc-Fe(100) leads. This figure shows that only for $s > 9$ the density of states in the center layer vanishes completely. However, one can see also that for $s > 6$ the slope of $n(\epsilon_F + i\delta)$ with respect to δ is positive, while it is slightly negative for $s = 3$. Fig. 3 on the other hand proves that although the density of states for $s = 3$ has not vanished, the slopes of the sheet resistances with respect to δ are of different sign. In the antiparallel alignment a “tunneling” situation is characteristic, while in the parallel alignment – in accordance with the simple density of states picture – metallic conductance is predicted. Clearly enough in such a case the magnetoresistance ratio is rather very big.

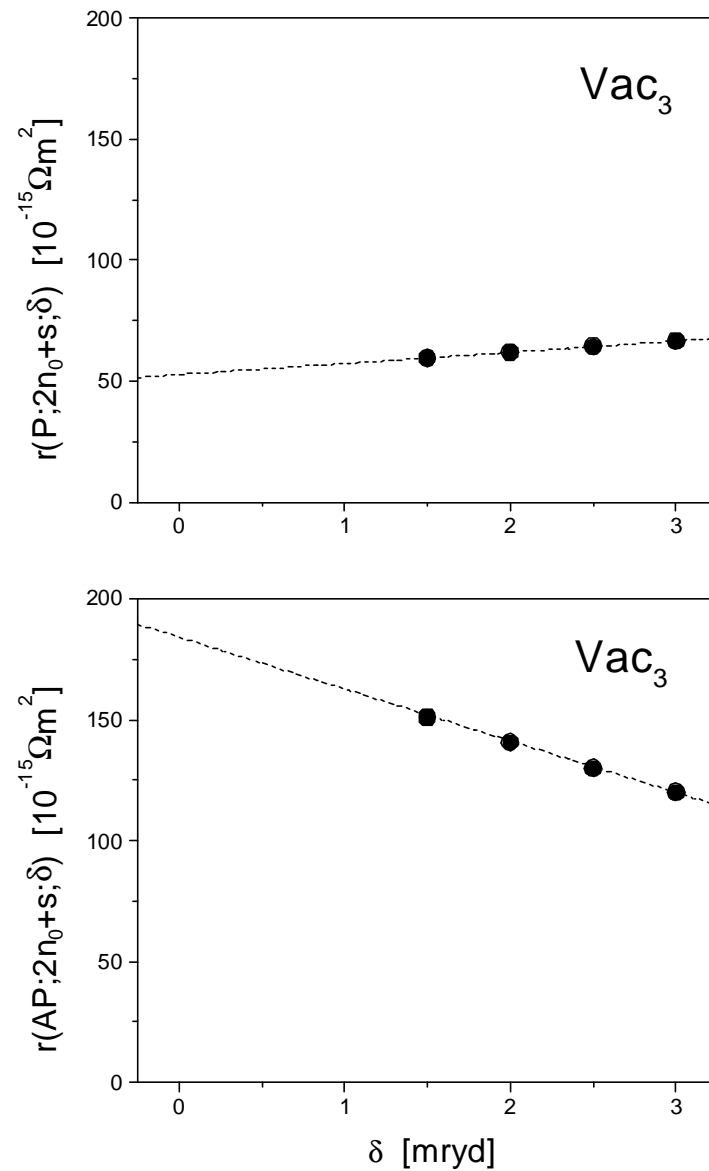


Figure 3: Analytical continuation of the sheet resistances $r(\mathcal{C}; 2n + s; \delta)$ in bcc-Fe(100)/Fe₁₂Vac₃Fe₁₂/Fe(100), $n \geq 11$, $s = 3$, to the real energy axis. Top: parallel configuration, bottom: antiparallel configuration. Full circles refer to calculated values, dotted lines to the corresponding linear fit. From ref. [18].

8 Where does the GMR effect in heterojunctions come from?

For illustrative purposes the layer-resolved sheet resistances can be defined,

$$r_i(\mathcal{C}; t; \delta) = \sum_{j=1}^t \rho_{ij}(\mathcal{C}; t; \delta) \quad , \quad r_i(\mathcal{C}; t) = \lim_{\delta \rightarrow 0} r_i(\mathcal{C}; t; \delta) \quad , \quad (40)$$

where t is again the total number of atomic layers considered. It is important to note that only the sum over these layer-resolved sheet resistances,

$$r(\mathcal{C}; t; \delta) = \sum_{i=1}^t r_i(\mathcal{C}; t; \delta) \quad , \quad r(\mathcal{C}; t) = \lim_{\delta \rightarrow 0} r(\mathcal{C}; t; \delta) \quad , \quad (41)$$

is well-defined. By partitioning the difference of the sheet resistances

$$\Delta r(t) = r(\mathcal{AP}; t) - r(\mathcal{P}; t) \quad (42)$$

with respect to the magnetic configurations into contributions arising from different parts of the heterostructure, namely the left and right electrodes (leads), L_{left} and L_{right} , the interface regions between electrodes and spacer, I_{left} and I_{right} , and the remaining spacer part S ,

$$\begin{aligned} \Delta r(t; \delta) &= \Delta r_{L_{left}}(t; \delta) + \Delta r_{L_{right}}(t; \delta) \\ &\quad + \Delta r_{I_{left}}(t; \delta) + \Delta r_{I_{right}}(t; \delta) + \Delta r_S(t; \delta) \quad , \end{aligned} \quad (43)$$

a very informative “picture” of where the magnetoresistance comes from can be given. Fig. 4 shows such a partitioning for the heterojunction $\text{bcc}(100)/\text{Fe}_n(\text{ZnSe})_s\text{Fe}_n/\text{Fe}(100)$. As can be seen in both kinds of termination the GMR effect is mostly determined by the Fe/ZnSe interfaces, indicating that the actual structure of the spacer is of little importance.

9 Interdiffusion at the interfaces

Very often interdiffusion at the interfaces occurs, usually causing the IEC and the magnetoresistance to decrease. An interesting case is $\text{bcc}(100)/\text{Fe}/\text{Si}/\text{Fe}(\text{bcc})$ since the regime of antiferromagnetic coupling is increased by interdiffusion, see Fig. 5. In this figure interface interdiffusion is restricted to a two-layer interdiffusion, meaning that the layers $\text{Fe}_c\text{Si}_{1-c}$ and $\text{Fe}_{1-c}\text{Si}_c$ form the interface, while all other layers remain “pure”. For the magnetoresistance (see Fig. 6), however, interdiffusion in this system is disastrous as Fig. 7 shows. Independent of the spacer thickness a two-layer interdiffusion corresponding to an interdiffusion concentration of about 15 - 20% almost kills the effect. This is the very reason of why up-to-now in this system only a very

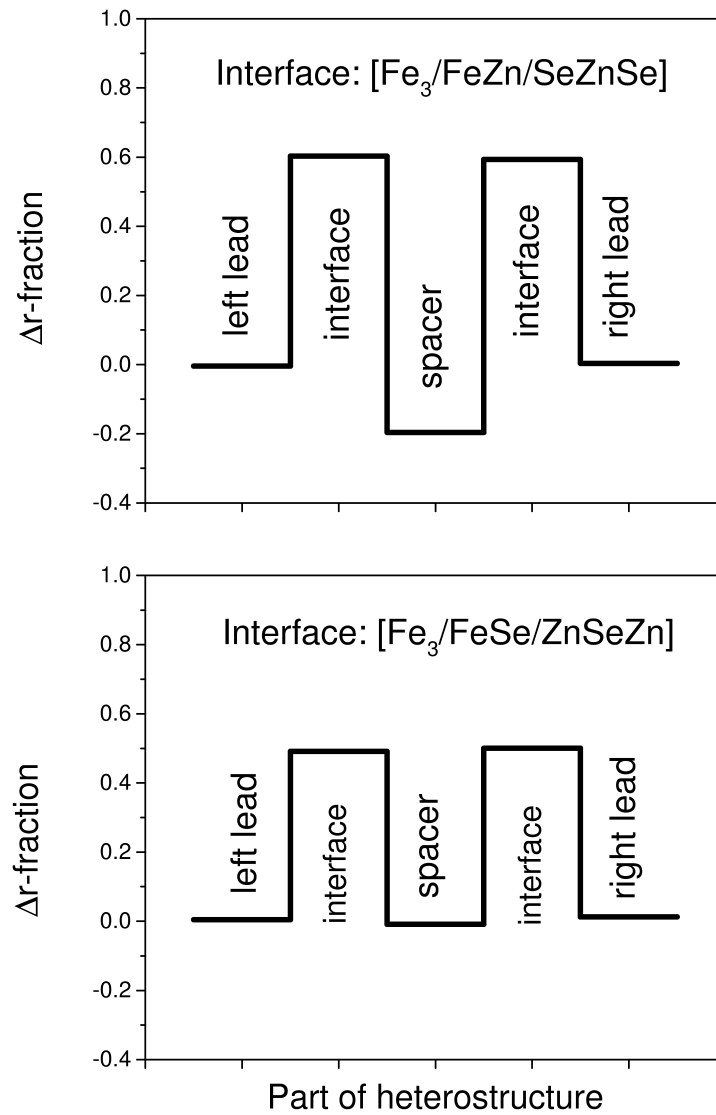


Figure 4: Normalized fractions of the difference in the sheet resistance between the antiferromagnetic and the ferromagnetic configuration in $\text{Fe}(100)/(\text{ZnSe})_{21}/\text{Fe}(100)$. The various regions of the heterostructure are given explicitly. From ref. [19].

small magnetoresistance ratio of less than 2% was found experimentally. Since however, the formation of ordered or disordered silicides at the interface is almost unavoidable, a Fe/Si/Fe heterojunction is probably a very bad candidate for a “TMR-device” (TMR: “tunneling magnetoresistance”).

10 Tunneling or not-tunneling?

In the top part of Fig. 8 an interesting case is displayed, namely the layer-resolved Madelung potentials in the “academic” heterojunction $\text{bcc-Fe}(100)/\text{Fe}_{12}\text{Vac}_{12}\text{Fe}_{12}/\text{Fe}(100)$ and modifications thereof in the interior part of the vacuum barrier. The lower part of this figure shows the corresponding changes in the parallel sheet resistance if the barrier is increased. As can be seen there is a very sharp increase of the sheet resistance as the value of the barrier increases. It should be noted that the open symbols in the top part of this figure correspond to the selfconsistent values, all other barrier heights are shifted by a constant with respect to the selfconsistent value. Fig. 9 presents the outcome of the opposite situation, namely reducing the value of the barrier. As can be seen (Fig. 9, top) the layer-resolved sheet resistances in the parallel configuration are reduced in the interior of the vacuum barrier as the barrier height is decreased. In the lower part of this figure the corresponding magnetoresistance ratios are depicted. As the barrier height is approaching the value of the Madelung potential in the semi-infinite leads (vertical line) a kink seems to develop separating the regime of metallic conducting from a regime of “tunneling”. This figure suggests that any heterostructure with an average barrier for a (non-metallic) spacer of about less than 2 eV will show a reasonable magnetoresistance ratio. Whether this is due to “tunneling” or very bad metallic conductance has to be argued in terms of the functional form of the sheet resistances with respect to the imaginary part of complex Fermi energies, see Fig. 3. Arguments in terms of (decaying) states, etc., unfortunately have little in common with the product of two Green’s function in the Kubo-Greenwood equation. Perhaps an experimentalist’s resumé [21], namely “*tunneling is rare*”, is the most witty answer to resolve the academic question of tunneling or not-tunneling.

11 Conclusion

It was shown that the present approach of evaluating CPP transport not only leads to a correct description of sheet resistances and magnetoresistance ratios for heterojunctions with in general interdiffused interfaces, but can be used also to discuss the role of interfaces. Furthermore, in terms of a physical interpretation of the imaginary part of the Fermi energy an essentially new aspect of the occurrence of tunneling can be given. In particular the lower part of Fig. 9 indicates that there is a kind of cusp that separates metallic from a “non-metallic” conductance, which seems to characterize also quite generally realistic heterojunctions between magnetic metals and semi- or non-conducting material.

Acknowledgement

The author is grateful for many discussions with V. Drchal, P. M. Levy, C. Sommers and L. Szunyogh. Investigations reported in this paper were financially supported in part by the Austrian Ministry of Science via special projects.

References

- [1] R. Kubo, “*Statistical-mechanical theory of irreversible processes. I. General theory and simple application to magnetic and conduction problems*”, J. Phys. Soc. Japan **12**, 570 (1957).
- [2] R. Kubo and S. J. Miyake, “*Quantum theory of galvanomagnetic effect at extremely strong magnetic fields*”, Solid State Phys. **17**, 269 (1965).
- [3] R. Kubo, M. Toda, and N. Hashitsume, *Statistical Physics II: Nonequilibrium Statistical Mechanics*, Springer Verlag, Berlin, 1985.
- [4] D. A. Greenwood, “*The Boltzmann equation in the theory of electrical conduction in metals*”, Proc. Phys. Soc. **71**, 585 (1958).
- [5] E. Y. Tsymbal and D. G. Pettifor, “*Perspectives of Giant Magnetoresistance*”, Solid State Physics Vol. **56**, 113 - 237 (2001).
- [6] P. M. Levy and I. Mertig, “*Theory of Giant Magnetoresistance*”, Advances in Condensed Matter, Vol. 3 Science (Ed. by D.D. Sarma, G. Kotliar and Y. Tokura), Taylor & Francis, London and New York (2002).
- [7] H. Eschrig, *Fundamentals of Density Functional Theory*, B. G. Teubner Verlagsgesellschaft, Stuttgart, Leipzig, 1996.
- [8] P. Weinberger and L. Szunyogh, “*Perpendicular magnetism*”, Computational Materials Science **17**, 414 (2000).
- [9] P. Weinberger, *Electron Scattering Theory for Ordered and Disordered Matter*, Clarendon Press (Oxford University Press), 1990.
- [10] P. Weinberger, P.M. Levy, J. Banhart, L. Szunyogh and B. Úfalussy, “*Band structure and electrical conductivity of disordered semi-infinite systems*”, J. Phys. Cond. Matt. **8**, 7677 (1996).
- [11] P. Weinberger, “*Ab initio theories of electric transport in solid systems with reduced dimensions*”, Physics Reports, in press (2003).

- [12] P. M. Levy, Solid State Physics Vol. 47, eds. H. Ehrenreich and D. Turnbull (Academic Press, Cambridge, MA, 1994) pp. 367-462.
- [13] H. E. Camblong, P. M. Levy, and S. Zhang, “*Electron transport in magnetic inhomogeneous media*”, Phys. Rev. B **51**, 16052 (1995).
- [14] B. Nikolić, “*Deconstructing Kubo formula usage: exact conductance of a mesoscopic system from weak to strong disorder limit*”, Phys. Rev. B **64**, 165303 (2001).
- [15] P. Weinberger, L. Szunyogh, C. Blaas, and C. Sommers, “*Perpendicular transport in Fe/Ge heterojunctions*”, Phys. Rev. B **64**, 184429 (2001).
- [16] P. Weinberger, “*Exchange bias due to configurational magnetic rearrangements*”, Phys. Rev. B **65**, 014430 (2002).
- [17] H. J. F. Jansen, “*Magnetic anisotropy in density-functional theory*”, Phys. Rev. B **59**, 4699 (1999).
- [18] P. Weinberger, V. Drchal, J. Kudrnovsky, I. Turek, H. Herper, L. Szunyogh and C. Sommers, “*Aspects of magneto-tunneling drawn from ab-initio type calculations*”, Philos. Mag. B **82**, 1027 - 1045 (2002).
- [19] H. C. Herper, P. Weinberger, A. Vernes, L. Szunyogh, and C. Sommers, “*Electric transport in Fe/ZnSe/Fe heterostructures*”, Phys. Rev. B **64**, 184442 (2001).
- [20] H. Herper, P. Weinberger, L. Szunyogh, and C. Sommers, “*Interlayer exchange coupling, magnetic anisotropy and perpendicular electric transport in Fe/Si/Fe trilayers*”, Phys. Rev. B **66**, 064426 (2002).
- [21] J. J. Akerman, I. K. Schuller, J. M. Slaughter, and R. W. Dave, “*Tunneling criteria for magnetic-insulator magnetic structures*”, J. Appl. Phys. Lett. **79**, 1, (2001).

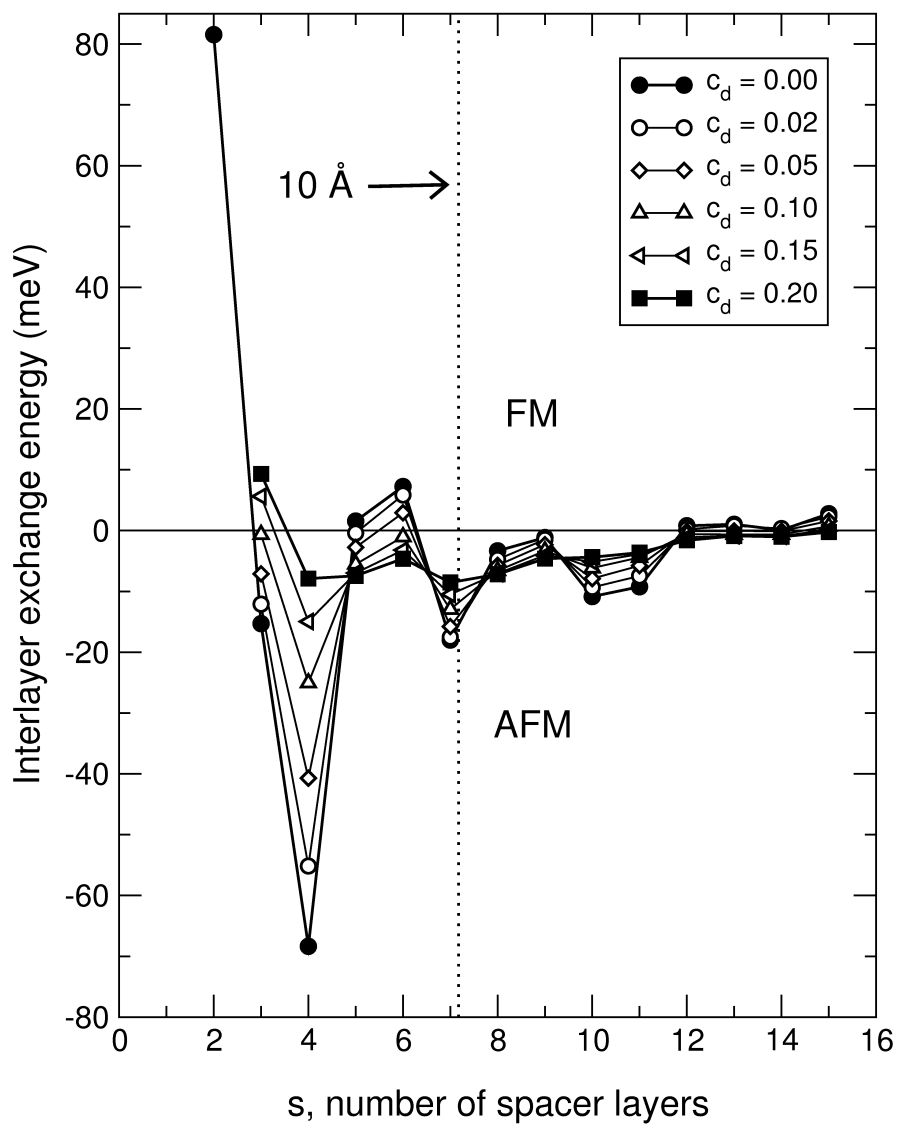


Figure 5: Changes of the IEC in $\text{bcc-Fe}(100)/\text{Si}_s/\text{Fe}(100)$ with respect to the number of spacer layers for different interdiffusion concentrations c_d . From ref. [20].

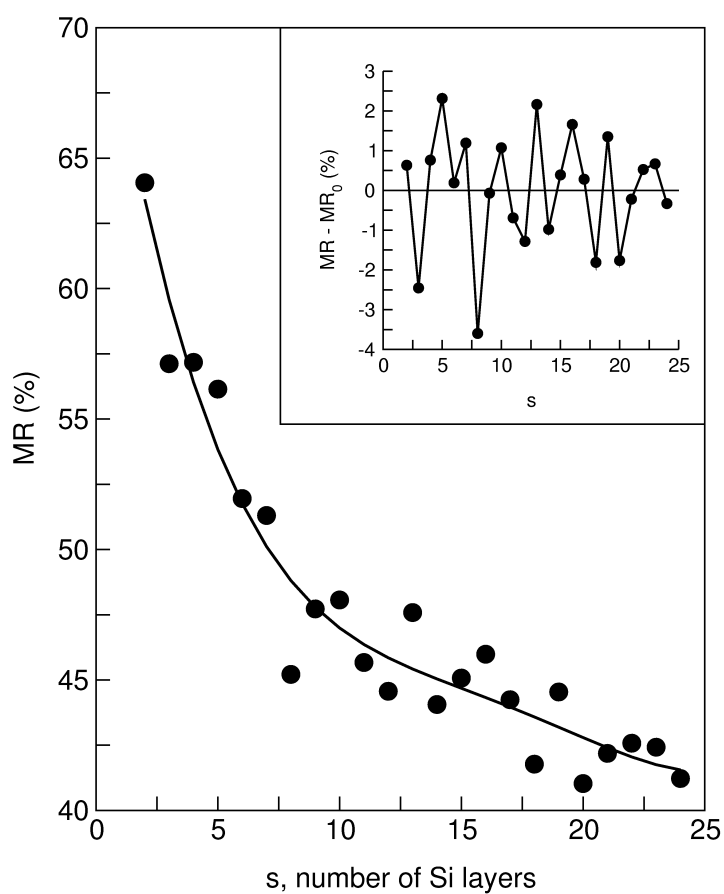


Figure 6: Magnetoresistance for Fe/Si_s/Fe trilayers versus the number of Si spacer layers s . The full line is a 4th order fit of the magnetoresistance to the data points. Inset: Difference between the calculated points and the fit depending on the number of Si layers. From ref. [20].

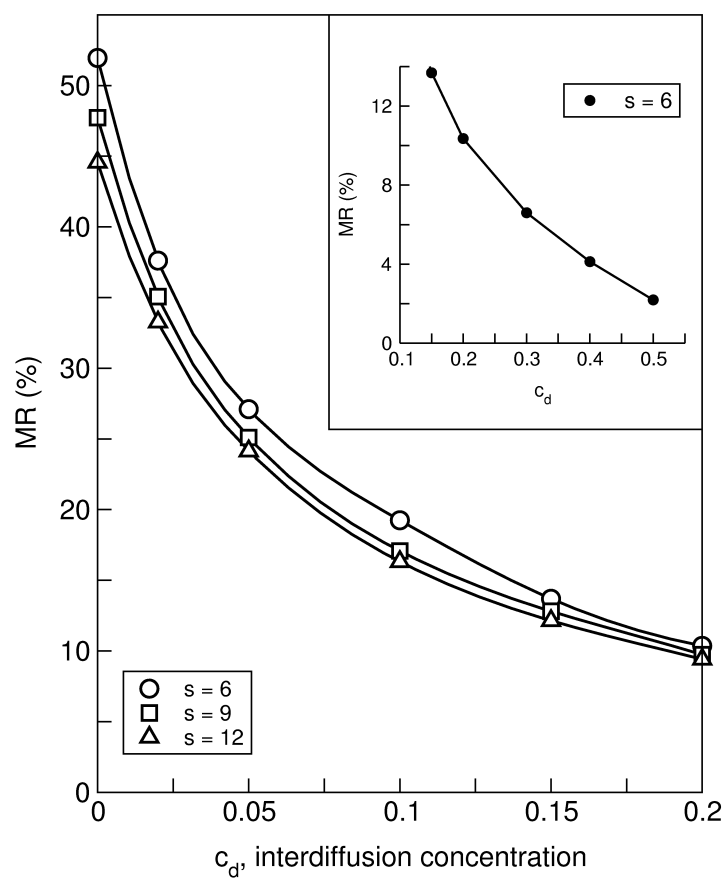


Figure 7: Dependence of the magnetoresistance on the interdiffusion concentration for Fe/Si_s/Fe systems. From ref. [20].

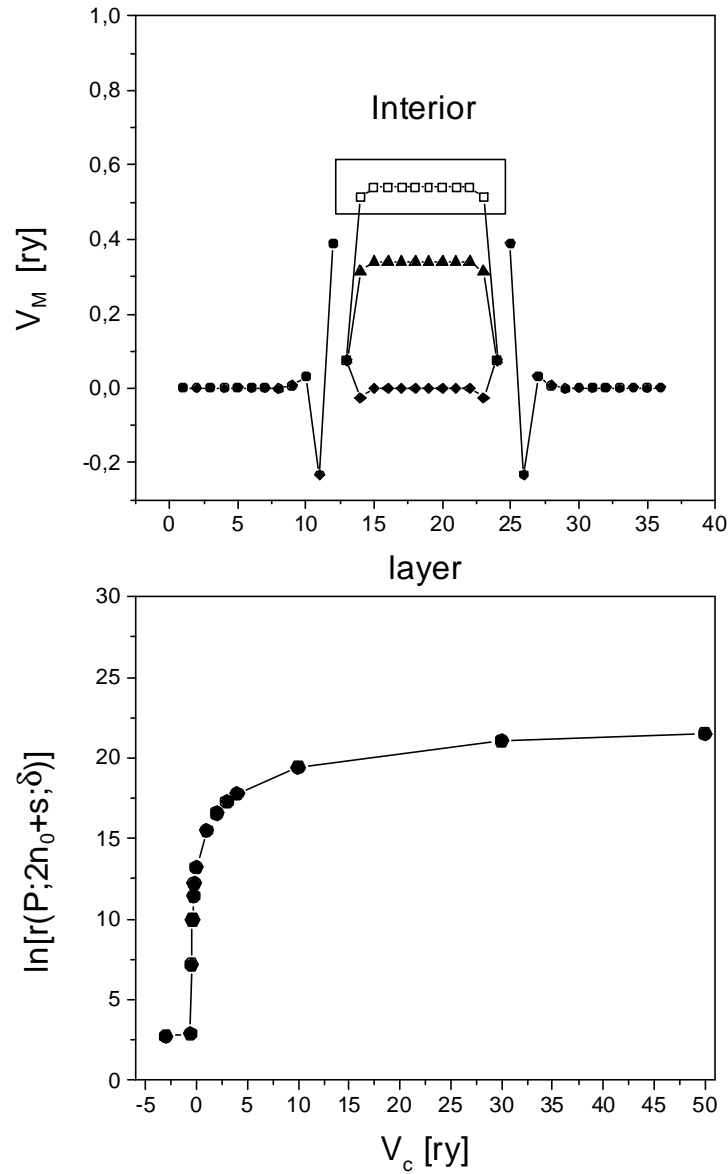


Figure 8: Top: Layer-resolved Madelung potentials and shifted potential barriers in the vacuum region of $\text{bcc-Fe}(100)/\text{Fe}_{12}\text{Vac}_{12}\text{Fe}_{12}/\text{Fe}(100)$. Circles: Fe; squares, triangles and diamonds refer to the vacuum region with $V_C = 0$, -0.2 ry and $-V_M$, respectively. Bottom: $\ln[r(\mathcal{P}; 2n + s; \delta)]$, $n \geq 11$, $\delta = 2$ mry, of $\text{bcc-Fe}(100)/\text{Fe}_{12}\text{Vac}_{12}\text{Fe}_{12}/\text{Fe}(100)$ as a function of V_C . V_M denotes the selfconsistently determined barrier height in the center layer of the vacuum region. From ref. [18].

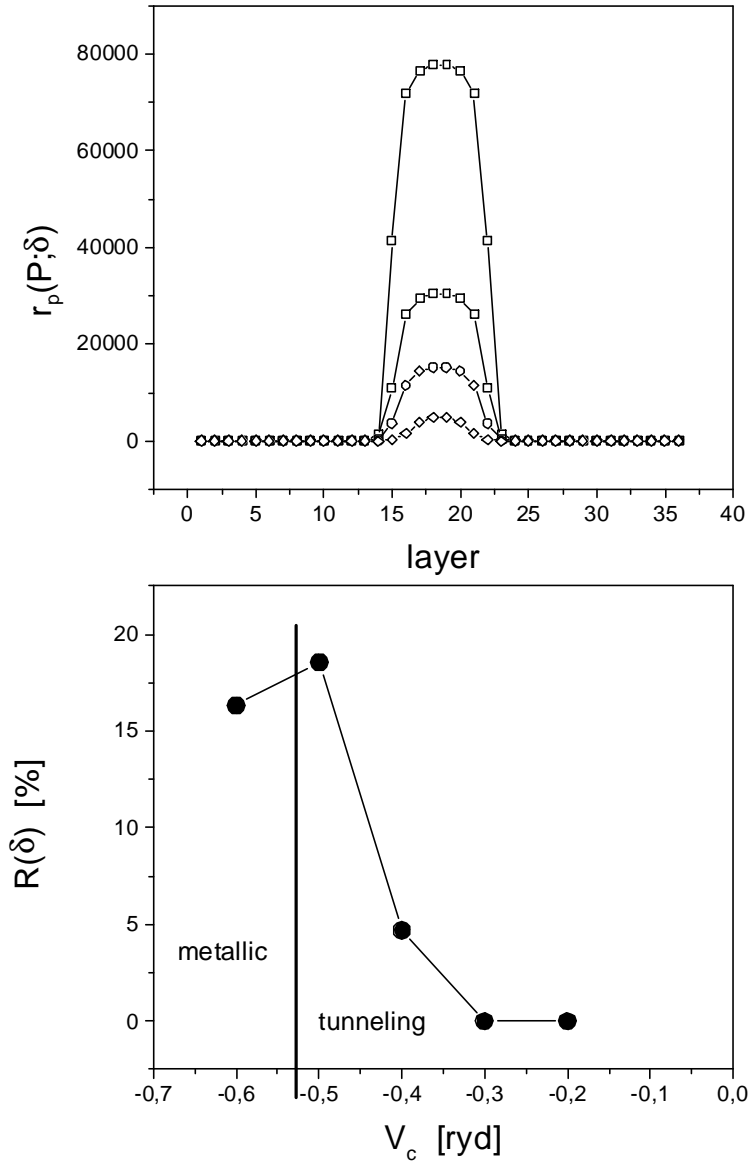


Figure 9: Top: Sheet resistance $r(\mathcal{P}; 2n_0 + s; \delta)$ (top) and magnetoresistance $R(2n_0 + s; \delta)$ (bottom), $\delta = 2$ mry, in bcc-Fe(100)/Fe₁₂Vac₁₂Fe₁₂/Fe(100) as a function of the constant shift V_C . In the top part squares, triangles, circles and diamonds refer to $V_C = 0, -0.2, -0.3$ and -0.4 ryd, respectively, in the lower part the regimes of metallic and tunneling behavior of electric transport are separated by the condition $V_M = -V_C$ (vertical line). V_M denotes the selfconsistently determined barrier height in the center layer of the vacuum region. From ref. [18].